1-1-2001

The effect of shrinkage and moisture in a numerical model of biomass pyrolysis

Mathew John Hagge
Iowa State University

The effect of shrinkage and moisture in a numerical model of biomass pyrolysis

By

Mathew John Hagge

A thesis submitted to the graduate faculty

in partial fulfillment of the requirements for the degree of

MASTER OF SCIENCE

Major: Mechanical Engineering

Major Professor: K.M. Bryden

Iowa State University

Ames, Iowa

2001

Graduate College

Iowa State University

This is to certify that the Masters thesis of

Mathew John Hagge

has met the thesis requirements of Iowa State University

Signatures have been redacted for privacy

TABLE OF CONTENTS

INTRODUCTION

The need for energy is driven by our ever-increasing demand for products and services. This reliance on energy has fueled the search for cost effective, readily available, and renewable sources of energy. In industrialized nations, interest in biomass comes from the potential to reduce carbon dioxide and sulfur emissions, as well as the elimination of waste products in agricultural applications. In developing countries, biomass is often the only readily available source of energy for cooking and heating. Heating and cooking can represent a much larger proportion of personal income in developing nations, and small improvements in efficiency can increase the standard of living dramatically. Fortunately, the needs of industrialized and non-industrialized nations coincide. Improving the efficiency and reducing the pollution of biomass combustion benefits all nations, by increasing the standard of living in poor nations, preserving forests, and reducing global pollution.

As with most renewable resources, better technology is needed to provide an attractive alternative to the more traditional energy sources of industrialized nations, such as coal, oil and nuclear power. Although there has been significant research on biomass combustion, it has received far less technology than the traditional sources of energy. A much better understanding is needed for biomass to become a viable source of energy.

This research represents an effort towards improving the understanding of the internal transport mechanisms that occur during the pyrolysis of biomass particles. A computational model has been used to investigate the pyrolysis of a shrinking biomass particle, as well as the effects of moisture within the solid matrix during pyrolysis.

Thesis Organization

This thesis investigates the importance of the shrinking solid matrix that occurs during pyrolysis of biomass particles. It contains a description of the characteristics and properties of wood that are relevant to this work and a brief description of previous modeling efforts. This introductory material is followed by a journal article that has been submitted for review. Additional conclusions and the direction of future work are also included

THE NATURE OF WOOD

Wood is composed of cellulose, hemicellulose, and lignin as well as a small amount of extractives, and ash forming materials. Cellulose typically accounts for approximately 50% of the dry weight of the wood. Extractives account for 5% to 10% of the dry weight of the wood, while ash content is less than 1% within the wood particle. The rest of the dry wood is made from varying amounts of hemicellulose and lignin. The cellulose ($C_6H_{10}O_5$) is a linear polymer that forms the structural component of the cell and is composed of a condensed polymer of glucose ($C_6H_{12}O_6$). The monomers contain hydroxyl groups that give cellulose a high affinity for water. Hemicellulose also contains bonded polymers, but is made from sugars other than glucose. Lignin ($C_{40}H_{44}0_6$) has a three dimensional structure which preserves the structure of the wood fiber, holding the cellulose and hemicellulose in a stable structure. The extractives are additional materials such as gums or oils that give the wood additional properties. The ash consists of calcium, potassium, magnesium, manganese and several oxides.

The structure of a wood particle has evolved to store and transport materials that are essential to the survival of a living organism. The basic building blocks of wood are long narrow fibers that can range from 1mm to 8 mm in length, with diameters varying from 20 to 30μm. These fibers are used to transport and store moisture, sap and other materials in softwoods.

Wood species are usually divided into hardwoods and softwoods. Softwoods are conifers while hardwoods loose their foliage annually. Hardwoods and softwoods have different chemical composition and structural properties. Softwoods fibers range from 3mm

to 8mm and are typically much longer than hardwood fibers, which average about 1mm in length. Softwoods typically contain 23% to 33% lignin by weight while hardwoods are composed of 16% to 25% lignin. The additional lignin serves to hold the much larger fiber together. Softwoods usually contain higher amounts of extractives. Hardwoods contain additional cells called pores that have a larger diameter (20 to 300μm) and are used for the movement of sap. Additional cells called rays are used in both hardwoods and softwoods to transport sap in the radial direction.

One of the many functions of the fibers is to store water within the cells. The amount of water within the wood can vary from over 50% on dry mass basis for green wood, to around 5% for fully dried wood. The hydrogen bonding within the fiber produces a strong attraction for water that holds the adsorbed water within the pores with increasing strength as the amount of moisture within the fiber decreases (Skaar 1988). At moisture contents above 30%, all of the fibers become saturated with water, and any additional water is unbound and free to move within the pores (Forest Products Laboratory 1987). Until the fiber saturation point is reached, the wood particle swells as the moisture content increases. Additional moisture content beyond the fiber saturation point does not cause any further swelling of the wood.

The combustion properties of wood are usually correlated to the proximate analysis, ultimate analysis, and the higher heating value of dried wood. The proximate analysis determines weight content of the volatile, char, and ash, while the ultimate analysis determines the weight fraction of carbon, hydrogen, oxygen, nitrogen, and sulfur. The volatile yield increases with temperature and heat flux by increasing the number of chemical bonds that are broken within the wood particle. The ultimate analysis remains fairly constant

for wood, with slightly higher amounts of carbon in softwoods due to the increased carbon content in the lignin and the extractives. Wood consists of 6% hydrogen (Petura 1979), 40% to 44% oxygen, and trace amounts of nitrogen and sulfur (Ragland, Aerts, and Baker 1991), and close to 50% carbon remaining. The higher heating value increases with carbon and hydrogen content, while decreasing with oxygen, nitrogen and ash. The respective quantities of cellulose, hemicellulose, lignin, extractives and ash will thus affect the higher heating value for a given species of wood. The higher heating value for softwoods to vary from 20 to 22 MJ/kg while hardwoods vary from 19 to 21 MJ/kg.

Drying

Drying occurs when the wood is heated. The rate of evaporation of the unbound water depends on the saturation pressure of the liquid as well as the partial pressure of the water in the wood pores. The water vapor has greater volume than the liquid water, and produces a greater pressure with the particle. The evaporation of water produces a pressure gradient within the particle that drives liquids and gases away from the drying region. Most of the gases and liquids are driven towards the surface of the particle, but some are driven towards the cooler region at the center of the particle. Additional energy is required to vaporize the bound water. In combustion experiments with logs (Bryden and Ragland 1997) observed that the inward migration of water was significant at low moisture contents (10%-15% as received), while the inward migration of water was limited at high moisture contents (35% to 45% as received).

Pyrolysis

The pyrolysis of wood is a chemical restructuring of the cellulose, hemicellulose, and lignin that occurs at elevated temperatures. Cellulose begins to pyrolyze at temperatures between 300°C and 350°C. Hemicellulose is pyrolyzed between 200°C and 300°C and lignin is pyrolyzed between 225°C and 475°C (Shafizadeh and Chin 1997). Species from the pyrolysis reactions include char, light hydrocarbons, tars, carbon dioxide and carbon monoxide. The volatile species produced by pyrolysis depend on the relative amounts of cellulose, hemicellulose, and lignin, as well as the rate of heating, with higher heating rates producing more volatile products.

In small particles, the biomass particle is at a nearly constant temperature from an evaluation of the Biot number, and the pyrolysis zone extends throughout the particle. As heat is transferred into the particle, the temperatures in the pyrolysis zone rise, and the rate of devolailization in the pyrolysis zone increases. The extent of the pyrolysis reactions thus becomes a function of the rate of heat transfer to the pyrolysis region, as well as the amount of volatiles remaining in the pyrolysis region. In very small particles, heat is transferred into the pyrolysis region at a much faster rate than the wood can devolatilize, and the pyrolysis reactions are controlled by the rate of the devolatilization of the wood.

In large particles, the pyrolysis zone ranges from 1mm to 3mm in length, and separates the unreacted wood from the external char layer (Ragland, Boerger, and Baker 1988). For these particles, the rate of internal heat transfer can be seen to control the heat transfer to the pyrolysis region from an evaluation of the Biot number. The rate of devolatilization is thus dependant on the rate of internal heat transfer, and pyrolysis occurs at

low temperatures, and over a long period of time. The minimum pyrolysis temperature is around 225°C (Chan, Kelbon, and Krieger 1985).

The heat of reaction for wood pyrolysis (Roberts 1971) has been reported to be slightly endothermic (370 kJ/kg) to exothermic (-1700kJ/kg). Smaller particles tend to produce endothermic values while larger samples produce exothermic values. Chan, Kelbon and Krieger (1985) note that the exothermic values in large particles may be due to secondary reactions of the primary pyrolysis products.

Char and Surface Reactions

The char and gas phase reactions have been turned off for this study, as the emphasis on this work is the pyrolysis reactions. A brief description has been included here because the effects of the assumptions in the numerical model on these reactions will be discussed later.

When wood is pyrolyzed, carbon atoms from the wood particle are bonded together in a nested honeycomb structure. The oxygen atoms, much of the hydrogen atoms, and some of the carbon atoms escape in the form of pyrolysis gases, which can easily pass through the honeycomb structure of the char layer. Due to the large surface area of the honeycomb structure, the pyrolysis gases are heated to the local temperature of the char layer.

Char combustion occurs when the surface of the char is exposed at elevated temperatures to gases including oxygen, carbon dioxide, hydrogen and water (Laurendeau 1978). The pyrolysis gases also react with oxygen in the external boundary layer. If the energy released from these reactions is sufficient to spark additional gas phase reactions, an attached or unattached flame will develop. A sustained flame requires a range of air to fuel

ratios, because not enough energy will be used for the gas phase reactions if the oxygen level is too low, and energy is used to heat the excess fuel, or if oxygen levels are too high, and energy is used to heat the excess air. If a flame zone is established, the oxygen will react in the flame zone before reaching the surface of the char. The carbon dioxide formed in the gas phase reactions will diffuse back towards the surface of the char, and the char and carbon dioxide reaction can become the dominant surface reaction (Makino, Araki, and Mihara 1994).

MODELING EFFORTS

As the ability to solve more and more complex problems has increased, there has been a progression of the pyrolysis and combustion models. These models attempt to account for the heat transfer within a biomass particle in conjunction with a specified reaction scheme. The simplest models use a single reaction and a uniform biomass material. More advanced models use multiple reactions, char and wood regions, and variable properties.

Previous Modeling

The first combustion model was present by Bamford, Crank and Malan in 1946. This model was developed in conjunction with an experimental setup that measured the temperature at the center of a flat sheet of wood that was exposed to burners on both sides. The model was developed by using the one-dimensional, time dependent heat conduction equation with a source term from a single pyrolysis reaction.

$$K\frac{\partial^2 T}{\partial x^2} - q\frac{\partial w}{\partial t} = C\rho\frac{\partial T}{\partial t}$$

The pyrolysis reaction was assumed to follow a first order Arrhenius relationship.

$$-\frac{\partial w}{\partial t} = kwe^{-E/RT}$$

and q is the heat release rate of the pyrolysis reaction on a mass basis.

Tinney (1965) modified this scheme by using different properties for wood and for char. Matsumoto, Fujiwara, and Kondo (1969) used the model of Bamford for plastics, and used thermal properties that depended on the amount of charring. They also introduced the

assumption of the gases are in local equilibrium with the char. Kung (1972) applied these assumptions to wood combustion. Kansa, Perlee, and Chaiken (1977) included the effects of a porous and permeable structure on the internal flow of pyrolysis gases by using Darcy's law on gases within the solid matrix. Kansa, Perlee and Chaiken recognized the need for secondary pyrolysis reaction when their model produced good results at low surface heating, but did not agree with experimental data at high surface heating rates.

Several researchers have developed models for biomass pyrolysis (Alves and Figueiredo 1989, Di Blasi 1995, Di Blasi 1996, Melaaen and Gronli 1997, Ragland, Boerger and Baker 1988, Saastamoinen 1993, Simmons 1983, Chan, Kelbon and Krieger 1985). These models account for the transport phenomenon within the particle and present a simplified representation of the chemical reactions that occur during pyrolysis. The transport phenomena that are accounted for in these models include gas flow within the solid matrix of the particle in conjunction with energy conservation and solid and gas phase continuity. Most of these models assume one-dimensional heat and mass transport and local thermal equilibrium between the solid and gas species. Many of these models do not include char shrinkage, resistance to flow within the particle, moisture content, and recondensation of volatile species.

Recent Models

More recent models (Di Blasi 1993, 1995,1996, Melaaen and Gronli 1997, and Bryden 1998) use variable properties, Darcy flow within the particle, gas phase continuity,

solid phase continuity, and conservation of energy in a one-dimensional medium. Di Blasi (1994) also presented a two-dimensional model for wood combustion.

As the ability of computers to solve increasingly complex problems grows, there have been several attempts to remove some of the simplifications of the earlier models. Different researchers have used different ways to include the effects of a shrinking solid matrix during the pyrolysis reactions (Parker 1986,Di Blasi 1996, Bryden 1998). Several methods have also been used to account for moisture within the biomass particle (Simmons 1983, Ragland, Boerger and Baker 1988, Saastamoinen 1993, Chan, Kelbon, and Krieger 1985, Alves and Figueiredo 1989, Ouelhazi, Arnaud, and Fohr 1992, Melaaen and Gronli 1997). As the complexity and diversity of these models increases, there is a need for an understanding of the implications of using a particular modeling scheme on the predicted results for pyrolysis.

MODELING THE IMPACT OF SHRINKAGE ON THE PYROLYSIS OF DRY BIOMASS

A paper submitted to Chemical Engineering Science

Mathew J. Hagge and Kenneth M. Bryden*

Department of Mechanical Engineering

Iowa State University, Ames, IA 50011-2161 USA

ABSTRACT— A new method for modeling shrinkage of a biomass particle is presented and validated in a detailed wood pyrolysis model. This model is applied to particle half-thicknesses ranging from 5 μm to 2 cm, temperatures from 800K to 2000K, and shrinkage factors of 1.0 to 0.4. Internal temperatures, pyrolysis rates, and yields of tar, light hydrocarbons and char are presented. Based on the results results of the model, it is found that shrinkage has a negligible affect on pyrolysis in the thermally thin (Bi<0.2) and the thermally thick ($0.2 \leq Bi \leq 10$) pyrolysis regimes. However in the thermal wave pyrolysis regime (Bi>10) shrinkage affects both the pyrolysis time and the pyrolysis products. In the case of a large 2-cm half-thickness poplar particle, with a background temperature of 2000K, and a shrinkage factor of 0.4, inclusion of shrinkage reduces the pyrolysis time by 43%, increases the tar yield from 7% to 13%, decreases the light hydrocarbon yield from 66% to 60%, and decreases the char yield slightly.

Key words: modeling, biomass, pyrolysis, fire, shrinkage

* Corresponding Author: Kenneth M. Bryden, email kmbryden@iastate.edu, ph 1-515-294-3891,fax 1-515-294-3261.

Introduction

Biomass is an attractive fuel for power generation because it is a readily available renewable energy source that reduces sulfur dioxide and carbon dioxide emissions. The need for biomass fuels is driven by the need to reduce carbon dioxide emissions and the need to eliminate what has previously been considered a waste product in agricultural applications. An understanding of the chemical processes and transport mechanisms of biomass pyrolysis is important for many applications including optimization of boilers and large scale furnaces, determining forest fire behavior, and predicting the resistance of buildings to fire.

Current pyrolysis models apply conservation of mass, momentum, energy, and species to the pyrolysis process and include gas flow within the particle and multiple, competing two-step reactions. However, many of these models do not include the effects of shrinkage. Shrinkage of the solid matrix effects pyrolysis in several ways. The density of the pyrolysis products increases as a result of chemical restructuring during pyrolysis. The increased density and decreased distance across the pyrolysis region changes the temperature profile of the particle. A sharper temperature gradient causes heat to reach the interior of the particle more quickly, and the thinner and hotter char layer also effects the product yield. In this paper a new computational method for including shrinkage is presented, and this new method is used to examine the impact of shrinkage on the pyrolysis process.

Background

Several researchers have developed models for biomass pyrolysis (Alves and Figueiredo, 1989; Chan, Kelbon and Krieger 1985; Di Blasi, 1995; Di Blasi, 1996; Melaaen and Gronli, 1997; Ragland, Boerger and Baker, 1988; Saastamoinen, 1993; Simmons, 1983). The two primary aspects of these models are modeling the transport phenomenon and modeling chemical reactions during pyrolysis. Transport phenomenon in these models typically model gas flow within the solid matrix of the particle in conjunction with energy conservation and solid and gas phase continuity. Most of these models assume one-dimensional heat and mass transport and local thermal equilibrium between the solid and gas species. Many of these models do not include char shrinkage, resistance to flow within the particle, moisture content, and recondensation of volatile species.

In order to model the chemical reactions, a set of reactions needs to be chosen with appropriate reaction rates. Several different reaction schemes have been used to model the pyrolysis of biomass. The most advanced models currently available use multiple, competitive two-step reactions. These schemes generally decompose wood into char, light hydrocarbons, and one or more intermediates. These intermediates vary depending on the scheme and may be a solid, liquid or vapor. The most common primary reaction scheme decomposes wood into char, gas, and tar. Secondary reactions allow product yields to be a function of temperature, heating rate, and residence time within the particle. In her review, Di Blasi (1993a) recommends using tar cracking to lighter gases and tar repolymerization to char for the secondary reactions. This is the pyrolysis reaction scheme used for this paper.

Pyrolysis reaction rates are usually presented with Arrhenius temperature dependence and first order dependence on the mass of unreacted wood. Chan, Kelbon, and Krieger

(1985) present kinetic rate parameters for thermally thick combustion. The effects of the pressure wave within the particle and the resistance to flow within the particle were not included in determining these parameters. Kinetic parameters were also developed (Nunn et al., 1985) using experimental results based on gas, tar and char. These kinetic rate parameters are presented for the overall decomposition of gas and various subcomponents of gas but do not include rate parameters for the char or tar. Other researchers (Koufopanos et al., 1991) have also presented kinetic parameters for gas and tar as a group. Thurner and Mann (1981) found parameters by using particles small enough that mass transfer and secondary reactions were negligible. Based on this, the parameters of Thurner and Mann are used in this paper for the primary char, gas and tar reactions. Vapor phase decomposition of char is generally modeled as a homogeneous process that is proportional to the tar density, and has an Arrhenius type temperature dependence. The products of these reactions are light gases, light gases and a solid residue, or light gases and refractory condensable materials. There has been wide acceptance of the kinetic parameters of Liden, Berruti, and Scott (1988), that have been used by Di Blasi (1993b) to model pyrolysis reactions under a wide range of conditions. There is limited information available on the tar to char reaction. Di Blasi (1993b) estimates that this reaction occurs at $1/40^{th}$ the rate of the tar to gas reaction.

Shrinkage can occur for two reasons, due to a loss of water mass or as a result of the pyrolysis reactions. Shrinkage due to a loss of water mass typically accounts for a 5 to 10 percent reduction in particle size (Forest Products Laboratory, 1987). Shrinkage occurs in the char layer during the pyrolysis reactions because of a rearrangement of chemical bonds and the coalescence of graphite nuclei within the biomass particle. The amount of char shrinkage is a function of wood species, heat flux and temperature. Varying compositions of lignin,

cellulose and hemicellulose and other organic and inorganic materials result in different amounts of shrinkage for different species. Char shrinkage increases as the temperature increases, and also increase with the amount of time at a given temperature. Roughly one-half of the char shrinkage occurs during the rapid devolatilization of the biomass, with continued chemical rearrangement following the devolatilization process.

Three researchers have presented pyrolysis shrinkage models. Villermaux et al. (1986) presented a simplified combustion model for wood in which wood was modeled as a homogeneous particle with a constant density. The constant particle density was used in conjunction with a single first order reaction to determine a surface shrinkage rate. This simplified combustion model does not include separate char and wood species, internal flow, or competitive pyrolysis reactions. Parker (1986) presented a model that accounts for shrinkage, by means of a prescribed change in geometry at the surface of the particle. Di Blasi (1996) presented shrinkage model with three parameters accounting for solid shrinkage, changes in volatile fraction, and changes in wood porosity.

Parker's model (1986) is used to predict the heat release rates while flaming is occurring at the surface. The surface of the particle is assumed to contain no oxygen while flaming occurs. In this model, wood is composed of lignin, cellulose, and hemicellulose. First order kinetic parameters are determined for each of these components experimentally. The control volume is divided into two separate regions consisting of an exterior char layer and an internal section of virgin wood. The char layer is arbitrarily defined at the depth where 90% of the original mass in an isothermal section remains. At this point, the geometry of the particle changes and triangular fissures are formed. Surface recession occurs in the char layer and the virgin wood according to this modified geometry. The total area of the char

region is determined from known experimental char contraction coefficients both parallel and perpendicular to the surface. The net heat transfer from the external radiation and convection into the walls of the fissures is assumed to be just sufficient to prevent lateral heat and volatile flow due to the change in cross sectional area with depth, thus maintaining the assumption of a one-dimensional heat and mass transfer. Flow is not modeled within the particle and the transit time of the volatiles to the surface is neglected. The volatiles are assumed to be in thermal equilibrium with the char layer. Volatiles that reach the char layer escape and do not interact with the char layer.

The Di Blasi (1996) model is an extension of her earlier pyrolysis model that includes the effects of shrinkage for a one-dimensional biomass particle. This model uses a primary and secondary pyrolysis scheme, and variable solid densities. Shrinkage is defined as a function of three separate parameters (α, β, γ). The volume occupied by the solid and the gases continuously varies during pyrolysis, as does the total volume. The volume occupied by the solid decreases linearly with wood mass and increases with char mass multiplied by the solid shrinkage factor (α).

$$\frac{\forall_S}{\forall_{WO}} = \frac{M_W}{M_{WO}} + \frac{\alpha M_C}{M_{WO}} \tag{1}$$

The volume occupied by the volatiles varies both due to the fraction (β) of the solid left by the devolatization process, and due to a change in porosity of the wood. The porosity is assumed to vary from some initial value to some fraction of the initial value (γ). The total volume of gas can be expressed as

$$\forall_G = \eta\forall_{gi} + (1-\eta)\gamma\forall_{gi} + \beta(\forall_{WO} - \forall_S) \qquad (2)$$

where $\eta = \frac{M_W}{M_{WO}}$ and $\forall_{gi}$ is the original volume occupied by the gases.

The Di Blasi model was run for a 5-cm particle (2.5 cm computational domain) for three cases. The first case contained no shrinkage ($\alpha = \beta = \gamma = 1$). In this case the loss of solid volume is accompanied by a gain in gaseous volume, such that the total volume of the particle remains constant. In the second case ($\alpha = 1, \beta = 0, \gamma = 1$), any loss of solid mass results in shrinkage of the particle volume, with the gas volume remaining constant. The third case used $\alpha = 0.5, \beta = 0, \gamma = 0.5$. In this case, in addition to the shrinkage of the solid volume, both porosity and gas volume were reduced. This model found that shrinkage resulted in an decrease in pyrolysis time and changes in the pyrolysis product yield. This highlights the need for inclusion of shrinkage in pyrolysis modeling.

Each of these models has strengths and weaknesses. The model of Parker accounts for shrinkage by changing the particle geometry at the exterior of the particle. One benefit of this model is that differing amounts of shrinkage in the tangential and radial direction can be specified, although there is no experimental basis for the proposed geometry. Parker does not account for the different physical properties of char and wood. The change in geometry occurs at the location where 10% of the original mass of wood has been lost. This instantaneous change from biomass to char and the consequent instantaneous change in thickness does not allow for the continuous progression of char and biomass composition. Resistance to internal flow is not included, and the product yields can not be determined. Di

Blasi presents a shrinkage model for pyrolysis that accounts for heat, momentum, and mass transport. Internal gas flow is accounted for using Darcy flow with the permeability of the medium expressed as a function of char and wood content. With internal flow and a two step reaction scheme, Di Blasi was able to predict the products of pyrolysis. A continuous change in properties is based on the respective amounts of char and wood at a given location using a linear progression variable. The three-parameter model of Di Blasi provides increased flexibility. However, no experimental values are available for these parameters and it is not clear that the solid volume, volatile volume, and wood porosity are not independent of each other. The model presented in this paper uses experimentally available data for the parameters in a detailed pyrolysis model.

Description of the Mathematical Model

A shrinking, dry, wood slab of thickness L, subjected on one surface to a radiant heat flux is modeled. The one-dimensional wood slab is a porous solid, and the void volume is initially filled with humid air. External heat transfer by radiation from a fixed temperature external source is assumed to be much greater than that by convection. As the slab is heated, the differing effective conductivities between the unreacted, wood and the char and the shrinking solid matrix result in a thermal wave with steep temperature and species gradients. Material properties (e.g., void fraction, permeability, thermal conductivity, specific heat), volume occupied by the solid, pressure, and temperature all continuously change with time. Shrinkage of the slab occurs as a result of pyrolysis. Pyrolysis is based on a two-step, five-reaction model in which primary wood pyrolyzes to light hydrocarbons (gas), tar, and char;

and secondary pyrolysis reactions decompose tar to gas and char. The complete set of reaction parameters for pyrolysis is given in Table 1. Wood drying and pyrolysis occur within the porous solid. A small amount of the pyrolysis gases are driven inward by the pressure gradient within the particle. The majority of the gases pass through the char layer, and provide blowing at the surface.

The mathematical model accounts for conservation of mass, momentum, species, and energy within a shrinking element. The derivations start with an arbitrary differential element. Within this element exist unreacted wood, char, and various gas species. The following assumptions are made: 1) wood is a one-dimensional porous reacting media with a well defined surface free of cracking; 2) gas and solid are in local thermal equilibrium; 3) diffusive transport of species within the pores is negligible; 4) the inertial terms within the momentum balance equation are negligible and flow can be described using Darcy flow; 5) shrinkage occurs only in the radial direction. The first assumption is commonly used although there are few real cases where this can be justified. Thermal properties and transport properties vary with grain orientation. Thermal conductivity is 2-3 times greater in the lengthwise direction and permeability has been reported to be 10^4 to 10^6 times greater in the radial direction. Even though wood is an anisotropic media, significant insight can still be gained from a one-dimensional model while keeping computation time at a reasonable level. The second assumption is based on an evaluation of the Peclet number, Pe. The Peclet number can be interpreted as the ratio of the rate of heat transfer by convection to the rate of heat transfer by conduction (Kansa, Perlee and Chaiken, 1977) Similarly, it can be shown that the diffusive transport of species within the wood pores is negligible (Chan, Kelbon and Krieger, 1985). The inertial terms in the momentum balance can be shown to be negligible

based on the small diameter of pores, and a small Reynolds number (< 0.01) (Kansa, Perlee and Chaiken, 1977). Assumption five is based on the assumption of a one-dimensional media.

Shrinkage is defined as the ratio between the reduced dimension, L, and the original dimension, L_O. This is consistent with reported values of shrinkage during pyrolysis in the fire literature. Thus the shrinkage factor is defined as

$$f = \frac{\text{current dimension}}{\text{original dimension}} = \frac{\Delta y}{\Delta y_O} \tag{3}$$

Cracking is neglected and shrinkage is assumed to occur only in the direction of interest. Therefore Δx and Δz are constant. For wood, char, and moisture the density of the material is described using the apparent density

$$\rho_i = \frac{m_i}{\forall} \tag{4}$$

where $\forall$ is the overall volume of the solid matrix including gases, $\forall = \Delta y \cdot \Delta x \cdot \Delta z$. Therefore for solids

$$m_i = \rho_i \left(\Delta y \cdot \Delta x \cdot \Delta z\right) = \rho_i f \left(\Delta y_O \cdot \Delta x \cdot \Delta z\right) = \tilde{\rho}_i \left(\Delta y_O \cdot \Delta x \cdot \Delta z\right) \tag{5}$$

where $\tilde{\rho}_i$ is the uncorrected density, that is the density obtained if the shrinkage is not considered.

$$\tilde{\rho}_i = \rho_i \cdot f \tag{6}$$

For computational simplicity $\tilde{\rho}_i$ is the uncorrected density is used for solid phase species and for the gaseous species ρ_i the apparent density is used.

$$\rho_i = \frac{m_i}{\varepsilon \forall} = \frac{m_i}{\forall_g} \tag{7}$$

where $\forall_g$ is the volume of the gases within the solid matrix and ε is the void fraction. Therefore for gases

$$m_i = \rho_i \varepsilon f\left(\Delta y_O \cdot \Delta x \cdot \Delta z\right) \tag{8}$$

For solid phase species mass does not cross the cell boundaries, and the species conservation equation reduces to the mass rate of storage of species *i* within the element equals the mass rate of production of species *i* within the element. For wood this becomes

$$\frac{\partial\left(\rho_W f\left(\Delta y_o \cdot \Delta x \cdot \Delta z\right)\right)}{\partial t} = \dot{\omega}_W\left(\Delta y_o \cdot \Delta x \cdot \Delta z\right) \tag{9}$$

which becomes

$$\frac{\partial \tilde{\rho}_W}{\partial t} = \dot{\omega}_W \tag{10}$$

where

$$\dot{\omega}_W = -(k_1 + k_2 + k_3)\tilde{\rho}_W \tag{11}$$

Following the same discussion, the char and moisture balances can be written as

$$\frac{\partial \tilde{\rho}_C}{\partial t} = \dot{\omega}_C \tag{12}$$

$$\frac{\partial \tilde{\rho}_M}{\partial t} = \dot{\omega}_M \tag{13}$$

The conservation equation for the total mass within the gas phase can be obtained from

$$G_g(\Delta x \cdot \Delta z)\Big|_x - G_g(\Delta x \cdot \Delta z)\Big|_{x+\Delta x} - \frac{\partial m_g}{\partial t} + \dot{\omega}_g\left(\Delta y_o \cdot \Delta x \cdot \Delta z\right) = 0 \tag{14}$$

where G_g is the mass flux of the pyrolysis gases normal to the surface, $G_g = \rho_g v$. After substitution and dividing by the volume, the conservation equation for the total mass within the gas phase becomes

$$\frac{\partial(\varepsilon f \rho_g)}{\partial t} + f\frac{\partial G_g}{\partial y} = \dot{\omega}_g \tag{15}$$

The Darcy law and the ideal gas law are

$$v = -\frac{\phi}{\mu}\frac{\partial p}{\partial y} \tag{16}$$

$$\rho_g = \frac{pW_g}{RT} \tag{17}$$

where ϕ is the permeability and μ is the dynamic viscosity. Permeability is assumed to vary with composition of the solid.

$$\phi = \eta\phi_W + (1-\eta)\phi_C \tag{18}$$

where η is a reaction progress variable

$$\eta = \frac{m_W}{m_{W,o}} \tag{19}$$

additionally W_g is the mean molecular weight of the gases

$$\frac{1}{W_g} = \sum_i \left(\frac{Y_i}{W_i}\right) \tag{20}$$

Substituting the Darcy law and the ideal gas law into the conservation equation for the total mass within the gas phase and simplifying yields a description of pressure evolution within the solid

$$\frac{\partial}{\partial t}\left(\frac{\varepsilon f p W_g}{T}\right) + f\frac{\partial}{\partial y}\left(\frac{p W_g}{T}\frac{\phi}{\mu}\frac{\partial p}{\partial y}\right) = R\dot{\omega}_g \tag{21}$$

A more computationally tractable form of the equation is obtained by expanding and simplifying to eliminate the molecular weight of the gas, W_g, yielding

$$\frac{\partial}{\partial t}\left(\frac{\varepsilon f p}{T}\right) + f\frac{\partial}{\partial y}\left(\frac{p}{T}\frac{\phi}{\mu}\frac{\partial p}{\partial y}\right) = R\left(\frac{\dot{\omega}_V}{W_V} + \frac{\dot{\omega}_L}{W_L} + \frac{\dot{\omega}_T}{W_T}\right) \tag{22}$$

In the same manner the conservation equation for tar can be obtained, this is

$$\frac{\partial}{\partial t}\left(\varepsilon f Y_T \rho_g\right) + f\frac{\partial}{\partial y}\left(Y_T G_g\right) = \dot{\omega}_T \tag{23}$$

The conservation equation for water vapor is

$$\frac{\partial}{\partial t}\left(\varepsilon f Y_V \rho_g\right) + f\frac{\partial}{\partial y}\left(Y_V G_g\right) = \dot{\omega}_V \tag{24}$$

A similar conservation equation could be obtained for light hydrocarbons; however, only two of three species conservation equations are needed and mass fraction of light hydrocarbons, is found using

$$Y_T + Y_V + Y_L = 1 \tag{25}$$

Conservation of energy is obtained in the same manner as the other conservation equations. Energy is transported in and out of the differential element by conduction, radiation, and mass flux. Conduction and radiation are accounted for by means of an effective thermal conductivity, λ_{eff} .

$$\lambda_{eff} = \lambda_{cond} + \lambda_{rad} \tag{26}$$

The contribution of conduction is obtained by summing the gas and solid contributions and assuming a linear variation between the wood and char conductivities, as follows:

$$\lambda_{cond} = \eta\lambda_W + (1-\eta)\lambda_C \tag{27}$$

Radiation heat transfer is accounted for through the use of an effective radiative contribution (Panton and Rittman, 1971)

$$\lambda_{rad} = \frac{\varepsilon}{(1-\varepsilon)}\sigma d_p 4T^3 \tag{28}$$

where σ is the Stefan-Boltzman constant and d_p is the effective pore diameter. The ratio of the thermal mass (ρc) of the wood char to the pyrolysis gas is approximately 650. Based on this, the energy stored in the gas phase is assumed to be negligible. The conservation of energy equation is

$$\frac{\partial\left(\tilde{\rho}_W i_W + \tilde{\rho}_C i_C + \tilde{\rho}_M i_M\right)}{\partial t} + f\frac{\partial\left(\left(Y_L h_L + Y_T h_T + Y_V h_V\right)\rho_g u\right)}{\partial y} = f\frac{\partial}{\partial y}\left(\lambda_{eff}\frac{\partial T}{\partial y}\right) + \sum \Delta h_i^o \dot{\omega}_i \tag{29}$$

where i is the internal energy. On the left side of the equation, the first term represents the change in the internal energy within the solid matrix and the second term represents the convective transport of energy from the gas phase species. On the right side, the first term represents conduction and radiation within the solid matrix and the second term represents the heat release from the pyrolysis reactions.

The conservation equations for the solid domain are solved using second-order accurate finite differencing. A moving boundary incorporates both char shrinkage and surface recession due to char gasification. The differenced equations developed are implemented in a Fortran based

computer code. The values and correlations used for the physical parameters are presented in Table 2. The number of grid points is chosen to provide good spatial resolution of the steep temperature and species gradients encountered. To achieve this, the number of grid points is varied depending on the thickness of the wood and the pyrolysis conditions. The number of grid points for the solid phase ranged from 21 to 1201. The time steps for the solid phase are chosen to ensure stability and accuracy of the solution. The time steps ranged from $1 \cdot 10^{-4}$ s to 1 s. Details of the numerical model are given in Bryden (1998).

The model was validated using the experimental work of Tran and White (1992). In these experiments wood blocks, built by gluing strips of wood together to form 15 cm × 15 cm × 6.4 cm blocks, were exposed on one of the 15 cm × 15 cm sides in air to a radiant heat flux. The dominant direction of the heat flux was tangential to the annual rings. The average charring rate as a function of heat flux for red oak, basswood, and southern pine is shown in Figure 1. The density, moisture content, and char shrinkage coefficients used in the model are those reported by Tran and White (1992) and are given in Table 3. The primary differences between these three woods are density and the char shrinkage. The less dense the wood, the smaller the mass of water to vaporize and the smaller the mass of wood to heat and pyrolyze, which results in faster charring rates. As the heat flux rises, the char shrinkage decreases due to less time at temperature, resulting in increased char thicknesses insulating the unreacted core from the flux, raising the surface temperature, and increasing the convective heat loss. As a consequence, the rise in the charring rate tends to flatten as the radiant heat flux increases. As shown, the match between the model and the experimental data is good, even though generalized wood pyrolysis kinetics are used in the model. Further details are available in Bryden (1998).

Modeling Results

The numerical model was used to examine the impact of shrinkage and particle size on the wood pyrolysis rate and regime. The pyrolysis cases discussed here are for a fixed background temperature that provides a radiant flux that dominates the heat transfer to the particle. Oxygen levels in the freestream are set to 0% with no gas phase or external char reactions. The half-thicknesses examined range from 50 μm to 2 cm. Background temperatures range from 800 to 2000 K, and moisture content was 0.1%. Shrinkage was varied from 0.4 to 1.0. Currently, biomass pyrolysis is commonly divided into thermally thin and thermally thick regimes, based on the internal and external rates of heat transfer (Pyle and Zaror, 1984). Thermally thin particles have a nearly uniform temperature across the particle. Thermally thick conditions occur whenever the thermally thin constant spatial temperature assumption cannot be used. This process can be extended to divide wood pyrolysis into three regimes based on internal and external heat transfer. These are 1) the thermally thin regime: this is the regime where internal resistance to heat flow is much less than the external resistance to heat flow (as used previously), 2) the thermally thick regime: the region in which internal and external resistance to heat transfer are approximately the same, and 3) the thermal wave regime: the regime where internal resistance to heat transfer is much greater than the external resistance to heat transfer. The Biot number can used to identify these regions with $\mathrm{Bi} \leq 0.2$, $0.2 \leq \mathrm{Bi} \leq 10$, and $10 \leq \mathrm{Bi}$ corresponding to the thermally thin, thermally thick, and thermal wave regimes, respectively (Bryden, Rutland and Ragland, 2001). In the thermally thin region for very small particles, external heat transfer

rate controls the time to heat up the particle. In the thermally thick region, both internal and external heat transfer are important. In the thermal wave the pyrolysis region is thin relative to the particle size and pyrolysis can be viewed as a reaction wave occurring in a very small region of solid matrix that travels forward at a varying velocity. In the thermal wave regime, this velocity is nearly constant for much of the pyrolysis process. Additionally, a thinner char layer decreases the residence time of the volatiles, limiting the secondary conversion of tar and increasing light hydrocarbon yields. The division of the thermally thick regime into two separate regimes permits the identification of the specific regimes in which moisture and shrinkage have different impacts. Shrinkage affects heat transport and volatile residence time, and has a significant impact in pyrolysis regimes where these processes are important. Shrinkage of the char matrix produces steeper temperature gradients. These steeper temperature gradients cause heat transfer to reach the interior of the particle much more rapidly and consequently decreases pyrolysis times.

A detailed quantitative comparison between experiment and the model is difficult because of the variances in property values, the simplified pyrolysis kinetics, and the effects of cracking. Rather, the model was used to examine the impact of shrinkage, to gain an understanding of how it can affect the pyrolysis process, and to understand under what pyrolysis or combustion conditions/regimes shrinkage must be considered. This can provide an improved qualitative understanding of pyrolysis and guide further research into modeling biomass pyrolysis and combustion.

In the thermally thin pyrolysis regime the particle temperature is uniform and pyrolysis occurs simultaneously throughout the particle. In this case there is no char

insulating the unreacted core. As a consequence shrinkage has only minor impact on pyrolysis time and product yield. Figures 2 and 3 show the temperature profiles and mass flux rate during pyrolysis of a thermally thin particle 100 μm thick (50 μm half-thickness) exposed to a background temperature of 1000 K. (Bi=0.05) This is similar to the pyrolysis of sawdust or finely ground agricultural residues (e.g. switchgrass leaves) in a suspension burner. The temperature across the particle is uniform and as expected there is no discernible difference between the case in which shrinkage is considered and the case in which shrinkage is not considered. The mass flux rate rises quickly and then falls. There is little residence time in the particle and the secondary pyrolysis reactions have little impact on the product yield. Because of this the ratio between tar and light hydrocarbon production changes very little during the pyrolysis process.

In contrast, in the thermally thick and thermal wave pyrolysis regimes, particle temperature is not spatially uniform. Rather there is an unreacted core surrounded by a layer of char separated by a thin pyrolysis reaction region. As pyrolysis proceeds the char layer grows at the expense of the unreacted core. The char layer impacts both the pyrolysis times and the pyrolysis products. As the char layer grows it insulates the particle reducing the heat transfer to the unreacted core and slowing the pyrolysis wave. Additionally, as the pyrolysis products flow through the char layer, the secondary pyrolysis reactions crack and repolymerize the tar. Shrinkage of the char layer causes a sharper temperature gradient, increasing heat transfer to the interior of the particle and raising pyrolysis temperatures. Within the thermally thick pyrolysis regime particle size is still relatively small. Because of this impact of char shrinkage on pyrolysis times and product yield is generally less than 6% and 3% respectively. Thermally thick pyrolysis is shown in Figures 4 and 5. Figure 4 shows

the temperature profile as a function of time for a 1.0 mm particle (0.5 mm half-thickness) exposed to a background temperature of 1600 K (Bi=1.9). While the thermally thick particle has a relatively large heat up time, temperatures within the particle vary by less than 200K. As a result, both the shrinking and non-shrinking particles have similar behavior for much of the life of the particle. As the char layer begins to develop, the shrinking char layer allows more rapid internal heat transfer. The increase in the rate of internal heat transfer increases the interior temperature of the particle while reducing surface temperatures. Figure 5 shows the mass flux for the 1.0 mm particle. The higher temperatures within the shrinking particle increase the rate of the primary pyrolysis reactions. At pyrolysis temperatures above 500°C, primary pyrolysis reactions produce very little light hydrocarbons and the increase in the rate of primary pyrolysis results in the increase in the rate of tar production. In the non-shrinking particle, increased residence times produce larger light hydrocarbon fluxes when a sufficient char layer has developed.

In the thermal wave regime the exterior of the particle heats up quickly, allowing pyrolysis to begin. A large temperature gradient develops within the particle and the pyrolysis front moves steadily towards the center of the particle. Figure 6 and 7 shows the temperature profiles and mass flux for a 1.0 cm (0.5 cm half-thickness) particle exposed to a background temperature of 1600 K (Bi=19) for shrinkage factors of 0.4 and 1.0 respectively. This case is similar to the pyrolysis of wood chips in a commercial packed bed furnace. The shrinking particle has a steeper temperature gradient across the pyrolysis reaction zone resulting in a thinner reaction region. This steeper temperature gradient within the shrinking particle develops because the rate of heat transfer in the thinner char region is increased relative to the time scale for the pyrolysis of the particle and heat transfer within the cold

unreacted core. The surface temperature is approximately 100 K lower for the shrinking particle. This occurs because of two factors. First there is less insulation from the char between the cold unreacted center and the surface. Second the higher pyrolysis rates result in higher flux rates of pyrolysis products, providing additional cooling for the char layer and reducing the temperature. This lowered surface temperature increases heat transfer at the surface, increasing the rate pyrolysis process. The higher heat transfer rates of the shrinking particle reduce the pyrolysis time from 20.2 sec to 15.1 sec. A reduction of 25%. As shown in Figure 7, initially both the shrinking and non-shrinking biomass particles have similar tar and light hydrocarbon yields. As a larger exterior char layer develops in the non-shrinking particle, the overall production rate of pyrolysis products in the shrinking particle is higher. Additionally, the ratio of tar to light hydrocarbons produced is much higher in the shrinking particle. This occurs because of the steeper temperature gradient within the pyrolysis reaction zone and the thinner, cooler char layer. In the shrinking particle the reaction zone is traveling inward at higher rate. This combined with a steeper temperature gradient raises the average temperature of pyrolysis region. This higher temperature leads to higher tar production from the primary pyrolysis reactions. In addition, as the pyrolysis products pass through the char layer the secondary pyrolysis reactions crack and repolymerize the tars to form light hydrocarbons and char. Within a thinner and cooler char layer of the shrinking particle secondary reactions rates are lower and less residence time is available for reaction reducing the conversion of tars. The secondary peak at the end of pyrolysis is a result of the increase in primary pyrolysis production at the center of the particle. Pyrolysis rates increase because there is no longer a cold core to slow the reaction wave.

As particle size increases the impact of shrinkage increases resulting in significantly reduced pyrolysis times and steeper temperature gradients in the pyrolysis reaction region. Figure 8 and 9 show the temperature profiles and mass flux rate in the thermal wave regime for a very thick, 4.0 cm (2.0 cm half-thickness), particle exposed to a background temperature of 1600 K (Bi=74) for a shrinkage factors of 0.4 and 1.0, respectively. For much of the pyrolysis time, all of the tar is converted to light hydrocarbons and char. As a result of the thinner and cooler char layer in the shrinking particle, more tar is able to escape before secondary conversion. Because of this, in addition to reducing the pyrolysis time by 43%, shrinkage increases the time over which tars are among the pyrolysis products by a factor of 3. As a consequence the overall tar yields are higher (11%) and light hydrocarbons are lower (10%) when shrinkage is present. Another impact of shrinkage is to reduce the fraction of the pyrolysis time in which there is a clear thermal wave and nearly constant mass flux.

Figures 10 through 12 summarize the affect of char shrinkage on the pyrolysis times of poplar for shrinkage factors of 0.4, 0.6, and 0.8 respectively. The effects of shrinkage increase with particle size and external temperature. The larger the particle the thicker the char layer. As a result shrinkage reduces the internal resistance to heat transfer to the unreacted core by reducing the insulating affect of the char. High external temperatures also increase the internal resistance within the particle relative to the external heat transfer rate. This increases the importance of the char layer and hence the importance of shrinkage. As shown, shrinkage does not have a significant affect on pyrolysis times for particles less than 0.5 mm in half-thickness. As shrinkage increases from 0.8 to 0.4 for a 2-cm half-thickness particle, the reduction of pyrolysis time increases from 12% to 43%. As the external radiant temperature increases from 800K to 2000K for smaller particles in the thermal wave regime,

the reduction in pyrolysis times increases by a factor of three (e.g. a 0.25 cm half-thickness particle with a shrinkage factor of 0.4 increases form 5% to 15%). In contrast, the reduction in pyrolysis times increases by 1.5 times for a larger particle as the external radiant temperature increases from 800K to 2000K (e.g. a 2.0 cm half-thickness particle with a shrinkage factor of 0.4 increases from 28% to 43%). This occurs because in thick particles the thicker char layers produce relatively large periods of nearly constant pyrolysis rate, lessening the impact of increasing temperatures and char thickness.

Figures 13, 14 and 15 summarize the impact of shrinkage on the pyrolysis products. As expected, in the thermally thin ($\mathrm{Bi} < 0.2$) and thermally thick ($0.2 \leq \mathrm{Bi} \leq 10$) regimes, where there are low temperatures and small particle sizes this impact is negligible. As previously noted, char shrinkage impacts the pyrolysis process in several ways, thinning the pyrolysis reaction region and increasing the pyrolysis temperatures, reducing the residence time of gases within the particle, and cooling the char layer due to the higher mass flux rates of pyrolysis products. Together, these effects significantly reduce the light hydrocarbon yield and increase the tar yield for particles in the thermal wave regime. Higher pyrolysis temperatures increase the tar yield and the shorter residence times and cooler char layer reduce the conversion of tar to light hydrocarbons. As shown at 800K this affect is small. For a 2-cm half-thickness particle with tar yield increases from 45% to 48% and decreasing light hydrocarbon yield from 23% to 20% as shrinkage increases from f_c =1.0 to f_c =0.4. At higher temperatures when secondary conversion of tar to light hydrocarbons is a key factor in product yield, shrinkage significantly alters the product yield. At 1400K, shrinkage reduces the light hydrocarbon yield in a 2-cm particle from 60% to 46%, while increasing the tar yield from 10% to 24% as shrinkage factor increases from f_c =1.0 to f_c =0.4. As temperature

rises further, the impact of shrinkage is reduced because even though the residence time is reduced, the higher temperatures within the char ensure that most of the conversion of tar to light hydrocarbons and tar is completed. At 2000K shrinkage reduces the light hydrocarbon yield for a 2-cm particle from 66% to 60% and increases the tar yield from 7% to 13% as shrinkage increases from f_c =1.0 to f_c =0.4. Char production remains relatively constant as shrinkage increases. Char production decreases with temperature and increases with particle size due to a small amount of repolymerization.

Conclusion

A new method for including char shrinkage in numerical modeling of biomass combustion has been presented. This char shrinkage model has been used in a detailed biomass pyrolysis model to examine the impact of char shrinkage on the pyrolysis process. The results of this study show that shrinkage has a negligible impact on pyrolysis times and product yield in the thermally thin (Bi<0.2) and thermally thick ($0.2 \leq \mathrm{Bi} \leq 10$). In the thermal wave regime (Bi>10) the impact of char shrinkage on pyrolysis times increases with temperature and particle size. At 2000K with a 2-cm particle shrinkage factors of 0.8, 0.6, and 0.4 reduce the pyrolysis times by 15%, 30% and 43% respectively. The impact of shrinkage on pyrolysis yield is more complicated. The reduced char thickness reduces the residence time for the pyrolysis gases reducing the secondary reactions, but as temperature increases this affect is minimized because the higher temperatures ensure a more complete conversion of tars to light hydrocarbons. As a consequence, the largest impact of shrinkage on product yield is at mid-ranged temperatures of 1400 - 1600K. With a shrinkage factor of

0.4 and a 2-cm half thickness, shrinkage increases the tar yield from 45% to 48%, 10% to 24% and 7% to 13% at temperatures of 800, 1400 and 2000K respectively. At the same time, the light hydrocarbon yield is reduced from 27% to 20%, 60% to 46%, and 66% to 60%, for temperatures of 800, 1400, and 2000K respectively.

References

Alves, S. S., and Figueiredo, J. L. 1989. A model for pyrolysis of wet wood. *Chemical.Engineering Science,* 44, 2861-2869.

Borman, G. L., Ragland, K. W. 1998. *Combustion Engineering.* McGraw-Hill, NewYork.

Bryden, K. M. 1998. *Computational Modeling of Wood Combustion.* Ph.D. Thesis, University of Wisconsin-Madison.

Bryden, K. M., Ragland, K. W., Rutland, C. J. expected 2001. Modeling thermally thick pyrolysis of wood. submitted to *Biomass and Energy.*

Chan, W. R., Kelbon, M., Krieger, B. B. 1985. Modeling and experimental verification of physical and chemical processes during pyrolysis of a large biomass particle. *Fuel,* 64, 1505-1513.

Di Blasi, C. 1993a. Modeling and simulation of combustion processes of charring and non-charring fuels. *Progress in. Energy and Combustion Science,* 19, 71-104.

Di Blasi, C. 1993b. Analysis of convection and secondary reaction effects within porous solid fuels undergoing pyrolysis. *Combustion Science and Technology,* 90, 315-340.

Di Blasi, C. 1995. Predictions of wind-opposed flame spread rates and energy feedback analysis for charring solids in a microgravity environment. *Combustion and Flame,* 100, 332-340.

Di Blasi, C. 1996. Heat, momentum, and mass transport through a shrinking biomass particle exposed to thermal radiation. *Chemical Engineering Science*, 51,1121-1132.

Forest Products Laboratory 1987. *Wood Handbook: Wood as an Engineering Material Agricultural Handbook 72*. U.S. Department of Agriculture, Washington, DC.

Kansa, E. J., Perlee, H. E., Chaiken, R. F. 1997. Mathematical model of wood pyrolysis including internal forced convection. *Combustion and Flame*, 29, 311-324.

Koufopanos, C. A., Papayannakos, N., Mashio, G., Lucchesi, A. 1991. Modeling the pyrolysis of biomass particles. Studies on kinetics, thermal and heat transfer effects. *The Canadian Journal of Chemical Engineering*, 69, 907-915.

Lee, C. K., Chaiken, R. F., Singer, J. M. 1976. Charring pyrolysis of wood in fires by laser simulation. *Sixteenth Symposium (International) on Combustion.* pp. 1459-1470. The Combustion Institute, Pittsburgh.

Liden, A. G., Berruti F., Scott D. S. 1988. A kinetic model for the production of liquids from the flash pyrolysis of biomass. *Chemical Engineering Communications*, 65, 207-221.

Melaaen, M.C., Grønli, M.G. 1997. Modeling and simulation of moist wood drying and pyrolysis. *Developments in Thermochemical Biomass Conversion* edited by A. V. Bridgwater and D. B. G. Boocock. pp. 132-146. Blackie, London.

Nunn, T. R., Howard, M. R., Longwell J. B., Peters W. A. 1985. Product compositions and kinetics in the rapid pyrolysis of sweet gum hardwood. *Industrial and Engineering Chemical Process Design and Development*, 24, 836-844.

Panton, R.L., Rittman, J.G. 1971. Pyrolysis of a slab of porous material. *Thirteenth Symposium (International) on Combustion.* pp. 881-891. The Combustion Institute, Pittsburgh.

Pyle, D.L., Zaror, C.A. 1984. Models for the low temperature pyrolysis of wood particles. *Thermochemical Processing of Biomass* edited by A. V. Bridgwater. pp. 201-216. Butterworths, London.

Ragland, K.W., Boerger, J.C., Baker, A.J. 1988. A model of chunkwood combustion. *The Forest Products Journal*, 38(2), 27-32.

Saastamoinen, J.J. 1993. Model for drying and pyrolysis in an updraft gasifier. *Advances in Thermochemical Biomass Conversion* edited by A. V. Bridgwater. pp. 186-200. Blackie, London.

Siau, F.F. 1984. *Transport Processes in Wood*, Springer Verlag, New York.

Simmons, W. W. 1983. *Analysis of Single Particle Wood Combustion in Convective Flow.* Ph.D. Thesis, University of Wisconsin-Madison.

Stull, D.R. 1971. *JANAF Thermochemical Tables, NSRDS-NBS 37.* US Government Printing Office.

TenWolde, A., McNatt, J.D., Krahn, L. 1988. *Thermal Properties of Wood and Wood Panel Products for Use in Buildings, DOE/USDA-21697/1.* Oak Ridge National Laboratory, Oak Ridge.

Thurner, F., Mann, U. 1981. Kinetic investigation of wood pyrolysis. *Industrial and Engineering Chemical Process Design and Development*, 20, 482-488.

Tran, H. C., White R. H. 1992. Burning rate of solid wood measured in a heat release rate calorimeter. *Fire and Materials*, 16, 197-206.

Villermaux, J., Antoine, B., Lede J. Soulignac, F. 1986. A new model for thermal volatilization of solid particles undergoing fast pyrolysis. *Chemical Engineering Science*, 41, 151-157.

White, R.H. 1988. *Charring Rates of Different Wood Species.* Ph.D. Thesis, University of Wisconsin-Madison.

Nomenclature

A	pre-exponential frequency factor
d_p	effective pore diameter
$\dot{e}$	rate of chemical energy release
E	activation energy
f	shrinkage factor
G	mass flux
h	heat transfer coefficient
Δh_k	heat of reaction for reaction k
Δh_i^o	heat of formation of species i
i	internal energy
k	rate constant
L_c	characteristic length
p	pressure
Q	external radiative heat flux
R	universal gas constant
t	time
T	temperature
W_i	molecular weight of species i
X	specific gravity
Y_i	mass fraction of species i

Greek

ε	void fraction
η	reaction progress variable
ϕ	permeability
φ	emissivity
λ	thermal conductivity
μ	dynamic viscosity
ρ	density
$\tilde{\rho}$	uncorrected density (see ref 1)
σ	Stefan-Boltzman constant
$\dot{\omega}_i$	mass rate of production of species i per unit volume

Dimensionless numbers

Bi	Biot Number
Py'	Second (External) Pyrolysis Number

Subscripts

C	char
cond	conduction
dry	dry
eff	effective
g	gas
L	light hydrocarbons
M	moisture
pyr	pyrolysis
r	recondensation
rad	radiation
T	tar
V	water vapor
W	wood
∞	Background

List Of Figures

Figure 11. Percent reduction in pyrolysis times as a function of temperature with a shrinkage factor of f_c =0.6 for several particle sizes.

Figure 12. Percent reduction in pyrolysis times as a function of temperature with a shrinkage factor of f_c =0.8 for several particle sizes.

Figure 13. Total light hydrocarbon production as a function of particle size for T=800K, T=1400K, and T=2000K ——— f_c = 0.4 and, - - - - - - f_c = 1.0.

Figure 14. Total tar production as a function of particle size for T=800K, T=1400K, and T=2000K ——— f_c = 0.4 and, - - - - - - f_c = 1.0.

Figure 15. Total char production as a function of particle size for T=800K, T=1400K, and T=2000K ——— f_c = 0.4 and, - - - - - - f_c = 1.0.

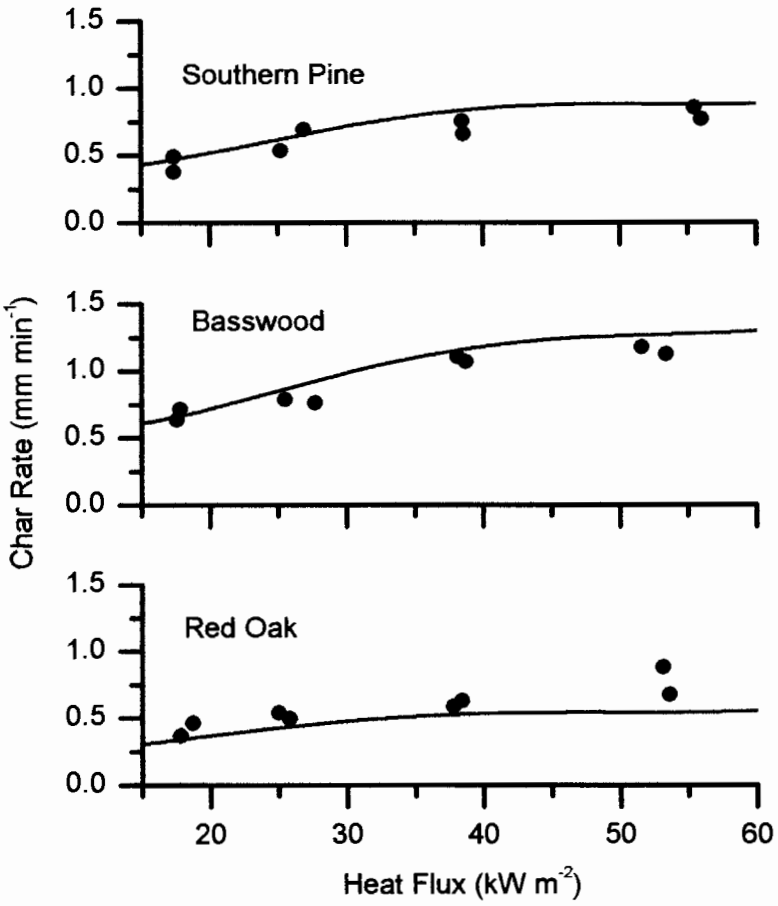
Southern Pine
Basswood
Red Oak
Char Rate (mm min-1)
Heat Flux (kW m-2)
0.0
0.5
1.0
1.5
20
30
40
50
60

Fig 1.

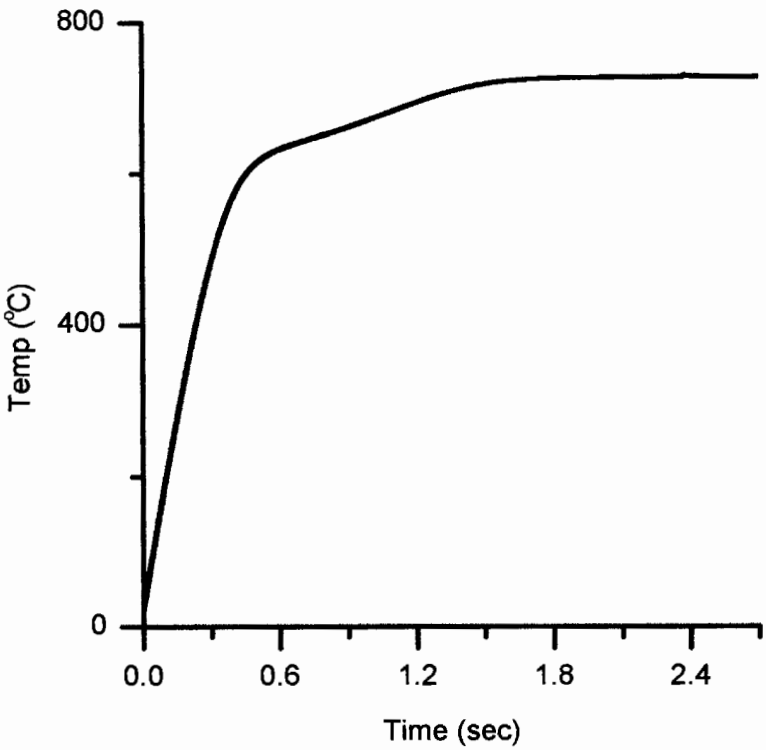

Fig 2.

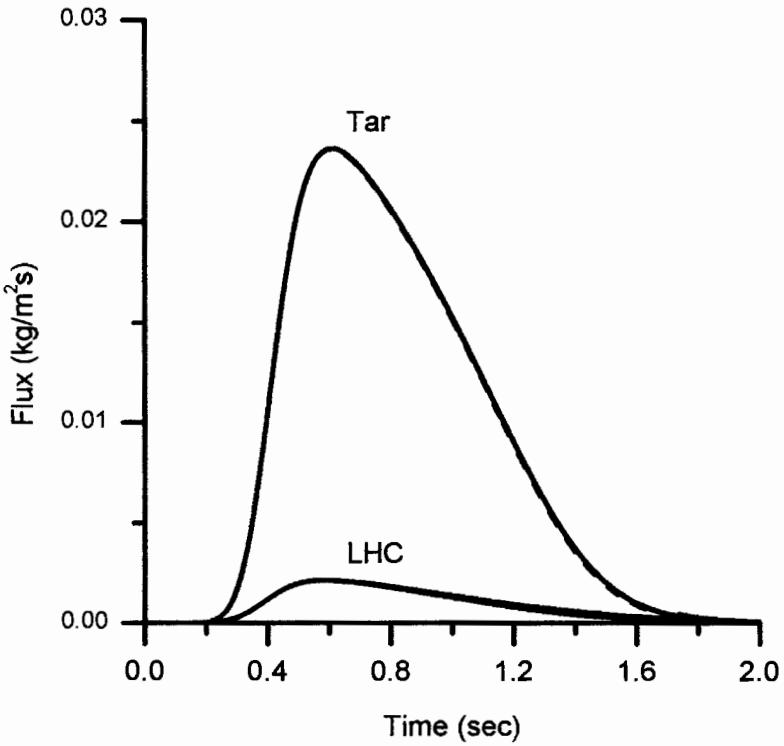

Fig 3.

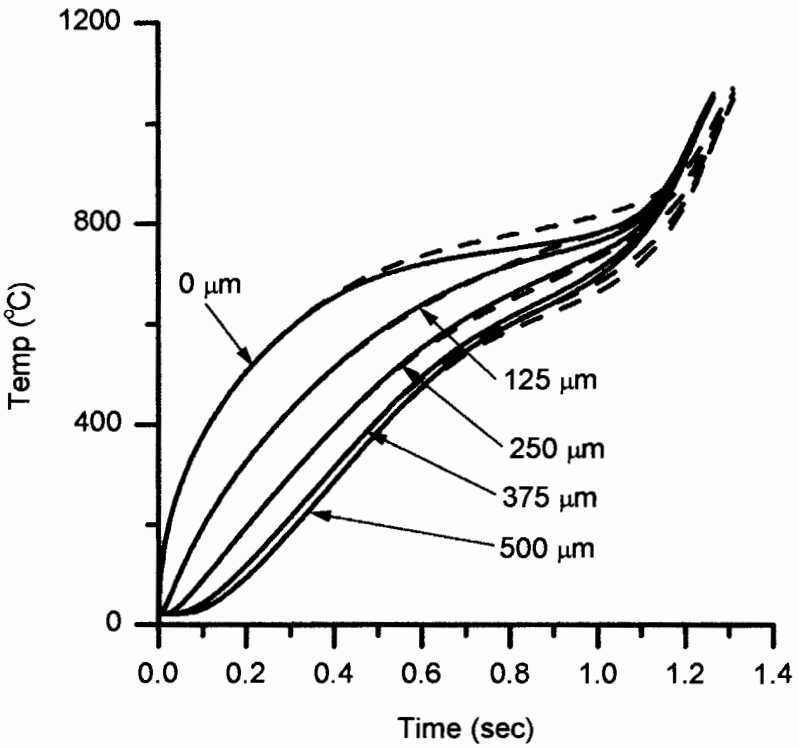
1200
800
400
0
Temp (°C)
0 μm
125 μm
250 μm
375 μm
500 μm
0.0
0.2
0.4
0.6
0.8
1.0
1.2
1.4
Time (sec)

Fig 4.

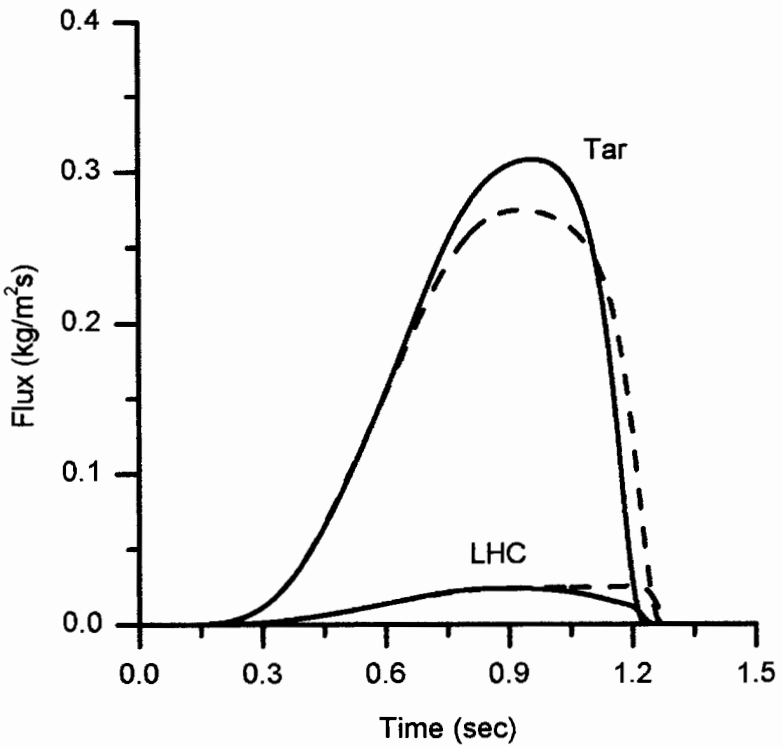

Fig 5.

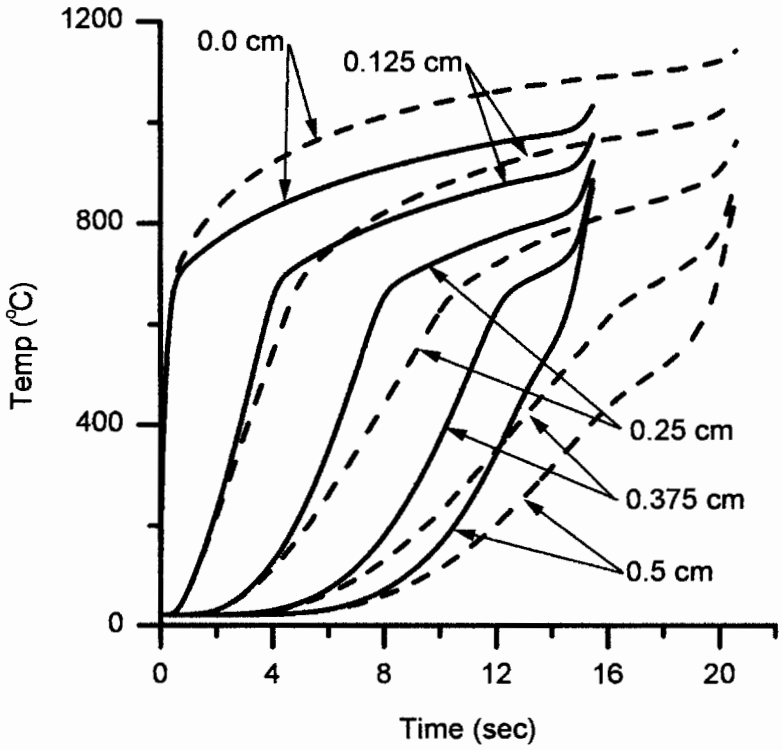
1200
800
400
0
Temp (°C)
0
4
8
12
16
20
Time (sec)
0.0 cm
0.125 cm
0.25 cm
0.375 cm
0.5 cm

Fig 6.

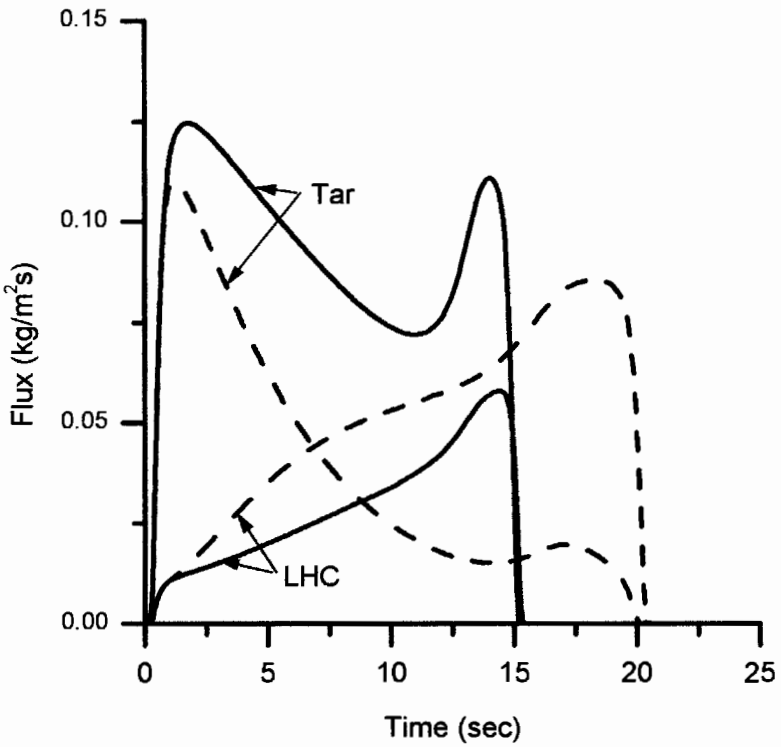

Fig 7.

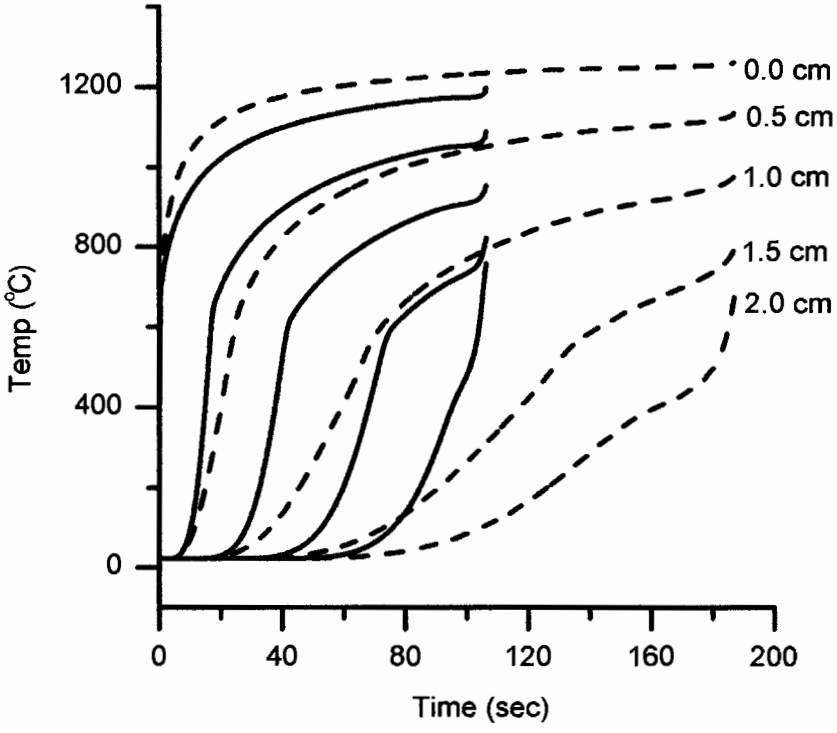
1200
800
400
0
Temp (°C)
0
40
80
120
160
200
Time (sec)
0.0 cm
0.5 cm
1.0 cm
1.5 cm
2.0 cm

Fig 8.

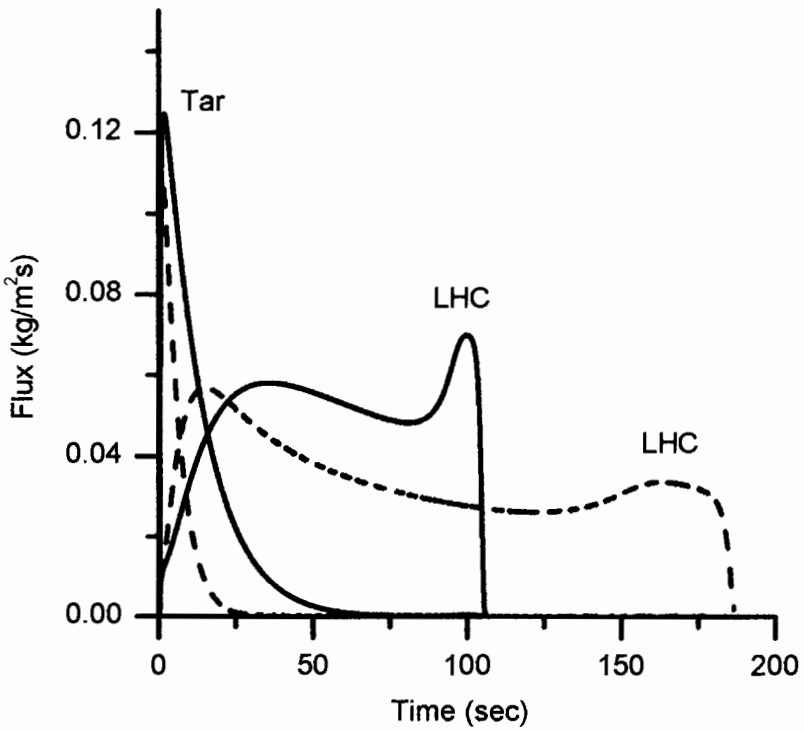

Fig 9.

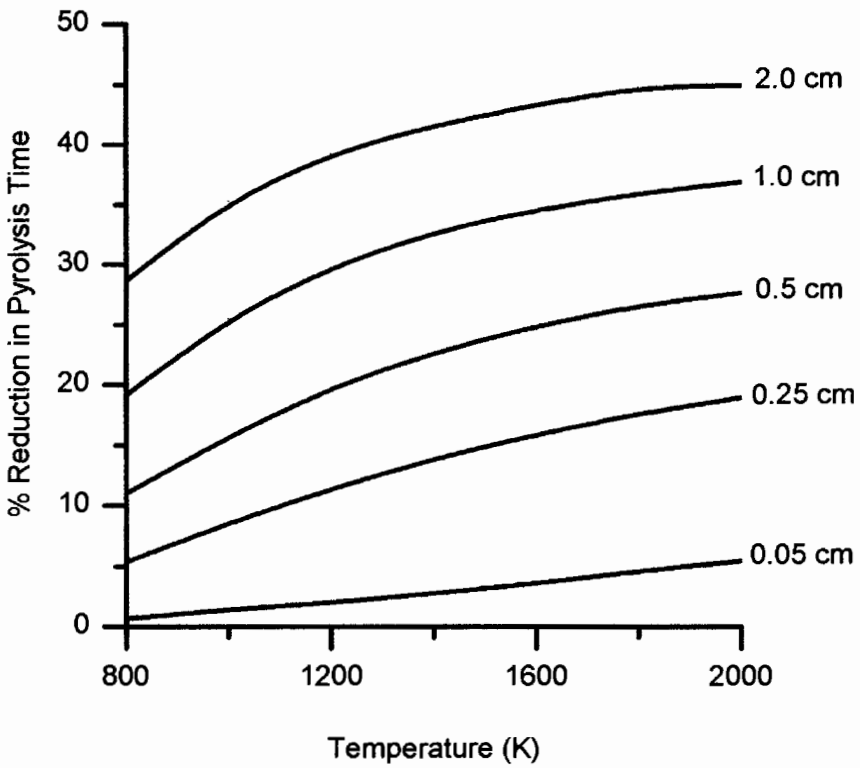
50
40
30
20
10
0
% Reduction in Pyrolysis Time
2.0 cm
1.0 cm
0.5 cm
0.25 cm
0.05 cm
800
1200
1600
2000
Temperature (K)

Fig 10.

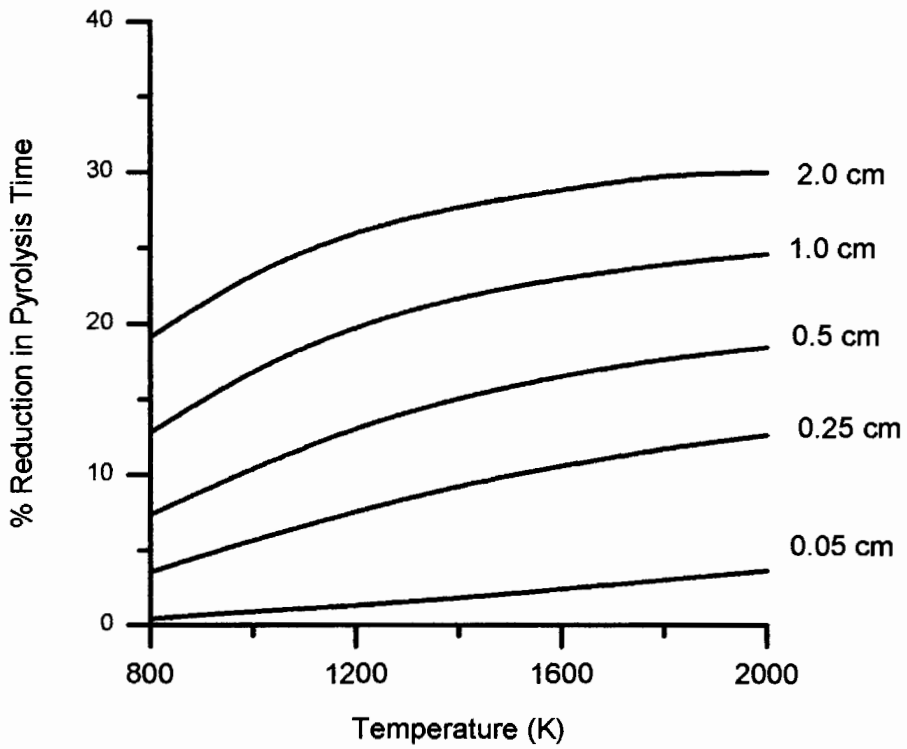
40
30
20
10
0
% Reduction in Pyrolysis Time
2.0 cm
1.0 cm
0.5 cm
0.25 cm
0.05 cm
800
1200
1600
2000
Temperature (K)

Fig 11.

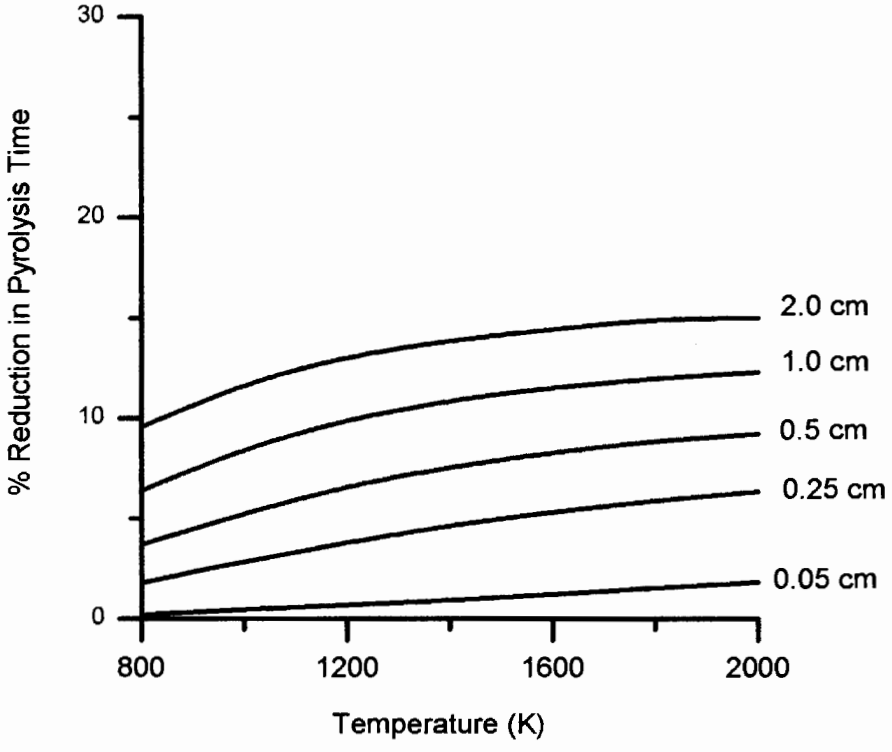
30
20
10
0
% Reduction in Pyrolysis Time
2.0 cm
1.0 cm
0.5 cm
0.25 cm
0.05 cm
800
1200
1600
2000
Temperature (K)

Fig 12.

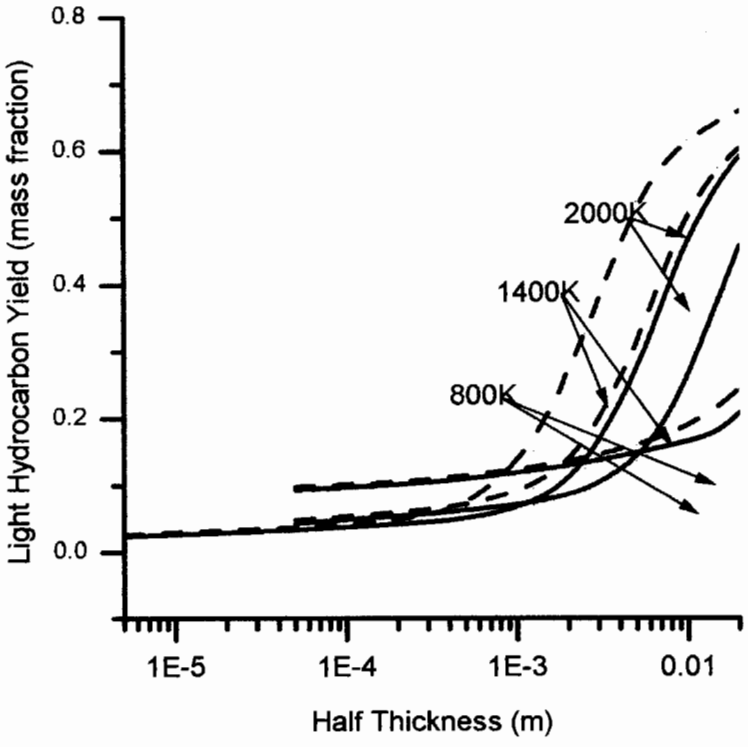
0.8
0.6
0.4
0.2
0.0
Light Hydrocarbon Yield (mass fraction)
2000K
1400K
800K
1E-5
1E-4
1E-3
0.01
Half Thickness (m)

Fig 13.

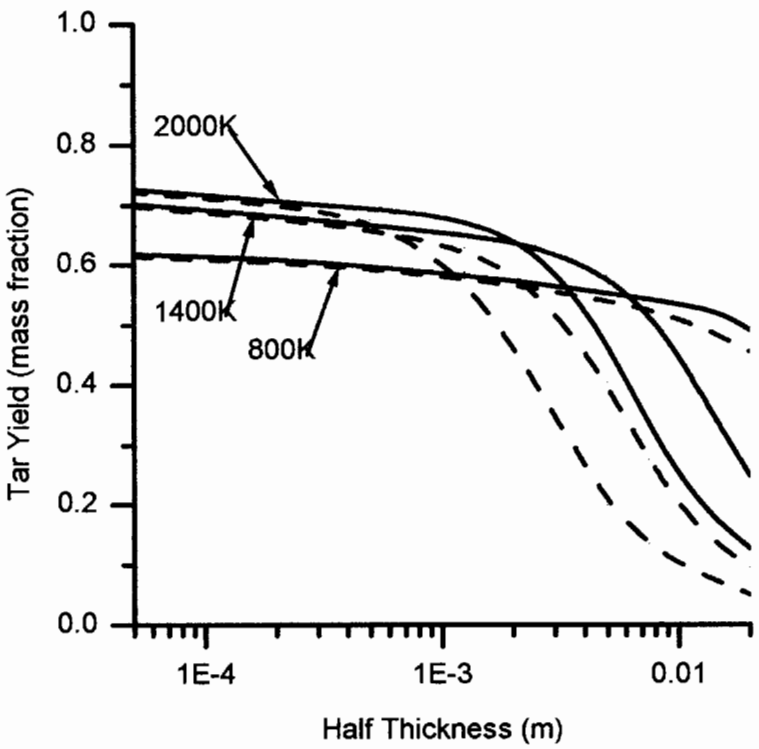
1.0
0.8
0.6
0.4
0.2
0.0
Tar Yield (mass fraction)
2000K
1400K
800K
1E-4
1E-3
0.01
Half Thickness (m)

Fig 14.

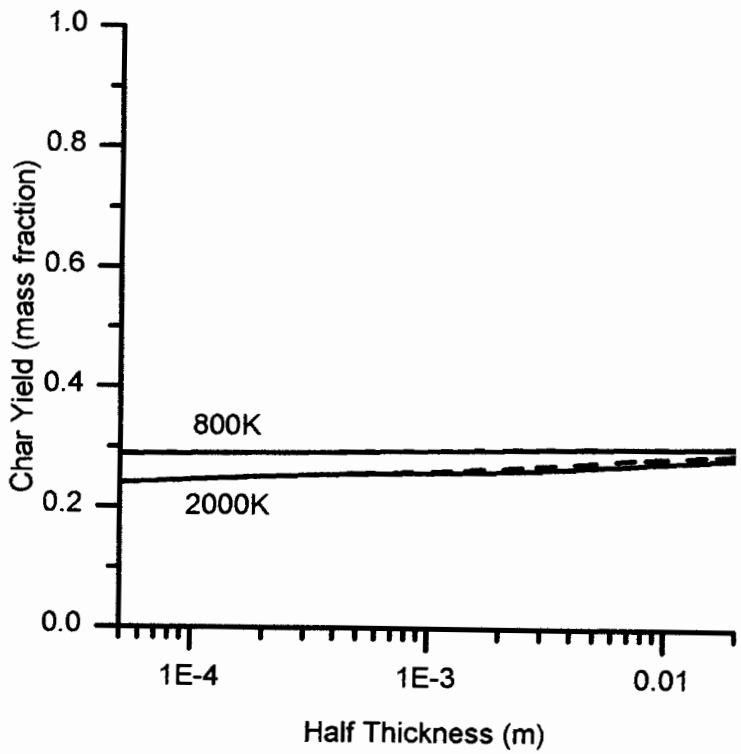
1.0
0.8
0.6
0.4
0.2
0.0
Char Yield (mass fraction)
800K
2000K
1E-4
1E-3
0.01
Half Thickness (m)

Fig 15.

Table 1. Parameters used for pyrolysis reactions.

Pyrolysis reactions					
Reaction	A (s^{-1})	E (kJ mol^{-1})	Ref	Heat of Reaction (MJ kg^{-1})	Ref
wood $\xrightarrow{k1}$ gas	$1.44 \cdot 10^4$	88.6	Thurner, Mann	-0.42	Di Blasi
wood $\xrightarrow{k2}$ tar	$4.13 \cdot 10^6$	112.7	Thurner, Mann	-0.42	Di Blasi
wood $\xrightarrow{k3}$ char	$7.38 \cdot 10^5$	106.5	Thurner ,Mann	-0.42	Di Blasi
tar $\xrightarrow{k4}$ gas	$4.28 \cdot 10^6$	107.5	Liden et al	0.04	Liden et al
tar $\xrightarrow{k5}$ char	$1 \cdot 10^5$	107.5	Di Blasi	0.04	Liden et al

Table 2. Values and correlations used.

Property	Correlation/Value	Ref
Void Fraction	$\varepsilon = 1-(\rho_w + \rho_C)/1500 - \rho_m/1000$	Siau
Permeability	$\phi = \eta\phi_W + (1-\eta)\phi_C$ where $\eta = m_W/m_{W,O}$	
	$\phi_w = 1\times10^{-2}$ darcys	Bryden
	$\phi_c = 1$ darcys	Bryden
Thermal Conductivity	$\lambda_{eff} = \lambda_{cond} + \lambda_{rad}$	
	$\lambda_{rad} = \varepsilon/(1-\varepsilon)\sigma\varphi_p d_p 4T^3$	Panton and Rittman
	$\varphi_p = 0.9$	assumed
	$\lambda_{cond} = \lambda_M + \eta\lambda_W + (1-\eta)\lambda_C$	
	$\lambda_W = 0.200\cdot X + 0.0238\ (\mathrm{W\ m^{-1}\ K^{-1}})$	Forest Product Lab
	$\lambda_M = X(0.0040\cdot M)\ (\mathrm{W\ m^{-1}\ K^{-1}})$	Forest Product Lab
	$\lambda_C = 0.105\ \mathrm{W\ m^{-1}\ K^{-1}}$	Lee et al
Specific Heat	$c_W = 0.003867(T-273.2)+0.1031\ (\mathrm{kJ\ kg^{-1}\ K^{-1}})$	TenWolde et al
	$c_C = 1.39+0.00036T\ (\mathrm{kJ\ kg^{-1}\ K^{-1}})$	Stull
	$c_{pyr} = 2.4\ \mathrm{kJ\ kg^{-1}\ K^{-1}}$	Bryden
	$c_M = 4.18\ \mathrm{kJ\ kg^{-1}\ K^{-1}}$	Borman and Ragland
Molecular Weight	$W_V = 18\times10^{-2}\ \mathrm{kg\ mol^{-1}}$	Borman and Ragland
	$W_L = 26\times10^{-2}\ \mathrm{kg\ mol^{-1}}$	Bryden
	$W_V = 110\times10^{-2}\ \mathrm{kg\ mol^{-1}}$	Bryden
Dynamic Viscosity	$\mu = 4.847\cdot10^{-7}T^{0.64487}\ (\mathrm{kg\ m^{-1}\ s^{-1}})$	Bryden
Heat Transfer Coefficient		
	$h_{rad} = \varphi\sigma\frac{1}{2}(T_s+T_\infty)(T_s^2+T_\infty^2)$ where $T_s = T_\infty$	Bryden

Table 3. Wood properties used in the model.

Species	Density ($g\ cm^{-3}$)	Ref	Shrinkage Factor (Drying)	Ref	Shrinkage Factor (Pyrolysis)	Ref
Basswood	420	Tran and White, 1992	0.934	Forest Product Lab, 1987	$0.354 + 0.003 \cdot Q$	Tran and White, 1992
Poplar	504	White 1988	0.954	Forest Product Lab, 1987	0.672	White 1988
Red Oak	660	Tran and White, 1992	0.956	Forest Product Lab, 1987	$0.446 + 0.005 \cdot Q$	Tran and White, 1992
Southern Pine	508	Tran and White, 1992	0.958	Forest Product Lab, 1987	$0.402 + 0.003 \cdot Q$	Tran and White, 1992

CONCLUSIONS

The transport mechanisms within a biomass particle are very complicated. Moisture and pyrolysis gases must travel through a complicated series of structures that were intended to provide nutrients throughout a living organism. The restructuring mechanisms that occur during the release of volatile products are not well understood. Property data at combustion level fluxes and temperatures are difficult to obtain. Certain properties and effects are impossible to model in one dimension. The computational modeling of biomass is a very difficult task that exceeds the limits of current technology.

The chemical restructuring that occurs during the pyrolysis reactions has a profound effect on the transport mechanisms within the biomass particle, decreasing pyrolysis times and altering the ultimate products of pyrolysis. Moisture present within the biomass particle increases the specific heat of the wood and cools the surface of the particle, increasing pyrolysis times and decreasing the rate of devolatilization.

Although the broad scale effects of these processes are well understood, the specific mechanisms by which they occur are not well known. The computational modeling of these internal processes has been limited by the inability to account for two and-three dimensional effects within the biomass particle. Cracking occurs to relieve the stresses caused by high temperature pyrolysis gases as well as the shrinking solid matrix. These cracks allow moisture and pyrolysis gases to escape much more easily. The increased surface area allows additional surface reactions and the biomass particle receives additional energy from exothermic gas phase reactions.

More research is needed into the exact nature of recondensation within the biomass particle and more research is needed to determine the relationship between the shrinkage and the heat flux as a function of time. To accurately model these effects as well as the anisotropic nature of biomass particles, these effects need to be extended to a two-dimensional model. The model should account for the changes in geometry of the particle as volatiles are released and cracking occurs. In addition, because the rate of diffusion of the gases in the external gas phase is dependent on the local geometry, the buoyant driven flow field needs to be determined from the particle geometry as well as the particle and gas phase temperatures.

REFERENCES

Alves, S.S., and Figueiredo, J.L., 1989, A model for pyrolysis of wet wood. *Chem.Engng Sci.* 44,2861-2869.

Bamford C.H., Crank J., and Malan D.H., 1946, The combustion of wood. Part I, *Proceedings of the Cambridge Philosophical Society* 42,166-182.

Borman, G.L., and Ragland, K.W., 1998, *Combust. Engng.* McGraw-Hill, NewYork.

Bryden, K. M., 1998, Computational modeling of wood combustion, PhD Thesis, University of Wisconsin-Madison.

Bryden, K.M., Ragland, K.W., 1997, Combustion of a single log under furnace conditions, *Developments in Thermochemical Biomass Conversion,* edited by A.V. Bridgwater and D.B.G. Boocock, Blackie Academic and Professional, London, 1331-1345.

Bryden, K.M., Ragland, K.W., and Rutland, C.J., expected 2001, Modeling thermally thick pyrolysis of wood, submitted to *Biomass and Energy.*

Chan, W. R., M. Kelbon, and B. B. Krieger, 1985, Modeling and experimental verification of physical and chemical processes during pyrolysis of a large biomass particle. *Fuel* 64,1505-1513.

Di Blasi, C., 1993a, Modeling and simulation of combustion processes of charring and non-charring fuels. *Prog. Energy and Combust. Sci.* 19,71-104.

Di Blasi, C., 1993b, Analysis of convection and secondary reaction effects within porous solid fuels undergoing pyrolysis. *Combust. Sci. Technology* 90,315-340.

Di Blasi, C., 1994, Processes of flames spreading over the surface of charring fuels: effects of the solid thickness, *Combust. Flame* 97,225-239.

Di Blasi, C., 1995. Predictions of wind-opposed flame spread rates and energy feedback analysis for charring solids in a microgravity environment. *Combust. Flame* 100, 332-340.

Di Blasi, C., 1996, Heat, momentum, and mass transport through a shrinking biomass particle exposed to thermal radiation. *Chem. Engng Sci.* 51,1121-1132.

Forest Products Laboratory, 1987, *Wood Handbook: Wood as an Engineering Material.* Agricultural Handbook 72, U.S. Department of Agriculture, Washington, DC.

Kansa, E.J., Perlee, H.E., and Chaiken, R.F., 1997, Mathematical model of wood pyrolysis including internal forced convection. *Combust. Flame* 29,311-324.

Koufopanos, C. A., N. Papayannakos, G. Mashio, and A. Lucchesi, 1991, Modeling the pyrolysis of biomass particles. Studies on kinetics, thermal and heat transfer effects. *Can J. Chem. Engng* 69,907-915.

Kung H.C., 1974, The burning of vertical wooden slabs, *Fifteenth Symposium (International) on Combustion*, The Combustion Institute, Pittsburgh, PA, 243-253.

Laurendeau N., 1978, Hetrogeneous kinetics of coal char gassification and combustion, *Progress of Energy Combustion Science* 4,221-269.

Lee, C.K., Chaiken, R.F., and Singer, J.M., 1976, Charring pyrolysis of wood in fires by laser simulation. In: Sixteenth Symposium (International) on Combustion., Pittsburgh: The Combustion Institute, p. 1459-1470.

Liden, A. G., F. Berruti, and D. S. Scott, 1988, A kinetic model for the production of liquids from the flash pyrolysis of biomass. *Chem. Engng Commun.* 65,207-221.

Makino A., Araki N., and Mihara Y., Combustion of artificial graphite in stagnation flow: estimation of global kinetic parameters from experimental results, *Combust. Flame* 96,261-274.

Matsumoto T., Fujiwara T., and Kondo J., 1969, Nonsteady thermal decomposition of plastics, *Twelfth Symposium (International) on Combustion*, The Combustion Institute, Pittsburgh, PA, 515-524.

Melaaen, M.C., and Grønli, M.G., 1997, Modeling and simulation of moist wood drying and pyrolysis. In: Bridgwater AV, Boocock DBG editors. Developments in Thermochemical Biomass Conversion. London: Blackie, p. 132-146.

Nunn, T. R., M. R. Howard, J. B. Longwell and W. A. Peters, 1985, Product compositions and kinetics in the rapid pyrolysis of sweet gum hardwood. *Ind. Engng Chem. Process Des. Dev.* 24,836-844.

Ouelhazi N., Arnaud G., and Fohr J.P., 1992, A two-dimensional study of wood plank drying. The effect of gaseous pressure below the boiling point, *Transport in Porous Media* 7,39-61.

Panton, R.L., and Rittman, J.G., 1971, Pyrolysis of a slab of porous material. In: Thirteenth Symposium (International) on Combustion. Pittsburgh: The Combustion Institute, p. 881-891.

Petura, R. C., 1979, Thermodynamic Data For Waste Incineration, The American Society of Mechanical Engineers, New York..

Pyle, D.L., and Zaror, C.A., 1984, Models for the low temperature pyrolysis of wood particles. In: Bridgwater AV editor. Thermochemical Processing of Biomass. London: Butterworths, p. 201-216.

Ragland, K.W., Boerger, J.C., and Baker, A.J., 1988, A model of chunkwood combustion. *Forest Products J.* 38(2):27-32.

Ragland, K.W., Aerts D.J., and Baker A.J., 1991, Properties of wood combustion analysis, *Bioresource Technology* 37,161-168.

Roberts, A.F., 1971, The heat of reaction during th epyrolysis of wood, *Combust. Flame* 17,79-86.

Saastamoinen, J.J., 1993, Model for drying and pyrolysis in an updraft gasifier. In: Bridgwater AV editor. Advances in Thermochemical Biomass Conversion. London: Blackie, p. 186-200.

Shafizadeh F., and Chin P., 1977, Thermal deterioration of wood, *Wood Technology*, ACS Press, Washington DC.

Siau, F.F., 1984, Transport processes in wood, Springer Verlag, New York, 1984.

Simmons W.W., 1983, Analysis of single particle wood combustion in convective flow, Ph.D Dissertation, University of Wisconsin-Madison.

Skaar, C., 1988, Wood-Water Relations, Springer Verlag, New York..

Simmons, W.W., 1983, Analysis of single particle wood combustion in convective flow. PhD Thesis, University of Wisconsin-Madison.

Stull, D.R., 1971, JANAF Thermochemical Tables, NSRDS-NBS 37. US Government Printing Office.

TenWolde, A., McNatt, J.D., and Krahn, L., 1988, Thermal properties of wood and wood panel products for use in buildings, DOE/USDA-21697/1. Oak Ridge National Laboratory, Oak Ridge.

Thurner, F. and U. Mann, 1981, Kinetic investigation of wood pyrolysis. *Ind. Engng Chem. Process Des. Dev.* 20,482-488.

Tinney E.R, 1965, The combustion of wooden dowels in heated air, Tenth Symposium (International) on Combustion, The Combustion Institute, Pittsburgh, PA 925-930.

Tran, H. C. and R. H. White, 1992, Burning rate of solid wood measured in a heat release rate calorimeter. *Fire and Materials* 16,197-206.

Villermaux, J., B. Antoine, J. Lede and F. Soulignac, 1986, A new model for thermal volatilization of solid particles undergoing fast pyrolysis. *Chem. Engng Sci.* 41,151-157.

White, R.H., 1988, Charring rates of different wood species. PhD Thesis, University of Wisconsin-Madison.